Available online at BCREC website: https://bcrec.id

Bulletin of Chemical Reaction Engineering & Catalysis, 18 (3) 2023, 420-441

Review Article

Organic Wastewater Treatment using Two-dimensional Graphene-based Photocatalysts: A Review

Kelvert Kong[1,a], Zhiying Zhu[1,a], Mukhamad Nurhadi[2], Sumari Sumari[3], Siew Fan Wong[4], Sin Yuan Lai[1,5*]

[1]School of Energy and Chemical Engineering, Xiamen University Malaysia, Jalan Sunsuria, Bandar Sunsuria, 43900 Sepang, Selangor Darul Ehsan, Malaysia
[2]Department of Chemical Education, Universitas Mulawarman, Kampus Gunung Kelua, Samarinda, 75119, East Kalimantan, Indonesia
[3]Department of Chemistry, Faculty of Mathematics and Natural Sciences, Universitas Negeri Malang, Jl. Semarang No. 5 Malang, 65145, Indonesia
[4]School of Engineering, Asia Pacific University of Technology and Innovation, Jalan Teknologi 5, Taman Teknologi Malaysia, 57000 Kuala Lumpur, Wilayah Persekutuan Kuala Lumpur, Malaysia
[5]College of Chemistry and Chemical Engineering, Xiamen University, 361005 Xiamen, China

Received: 31st August 2023; Revised: 16th September 2023; Accepted: 18th September 2023;
Available online: 21st September 2023; Published regularly: October 2023

Abstract

Photocatalysts have gained enormous attention in water decontamination due to their economic viable and intriguing properties. Recently, graphene-based semiconductors have become the sparkling star on the horizon of material science. The coupling of two-dimensional graphene and its derivatives (graphene oxide and reduced graphene oxide) with semiconductors could effectively enhance the efficiency in organic wastewater degradation under light irradiation. Hence, a collective study on this topic is necessary. Four types of graphene-based semiconductors, viz. titania, zinc oxide, cadmium sulfide, and bismuth oxychloride, are explored. Besides, synthesis approaches and properties of these photocatalysts are elucidated too. We hope this review could enable us to rationally design and harness the morphology, structure and electronic properties of these advanced materials.

Keywords: Organic pollutants; Wastewater treatment; 2D graphene-based photocatalysts; Photodegradation; Graphene oxide; reduced Graphene Oxide

How to Cite: K. Kong, Z. Zhu, M. Nurhadi, S. Sumari, S. F. Wong, S. Y. Lai (2023). Organic Wastewater Treatment using Two-dimensional Graphene-based Photocatalysts: A Review. *Bulletin of Chemical Reaction Engineering & Catalysis*, 18(3), 420-441 (doi: 10.9767/bcrec.20029)

Permalink/DOI: https://doi.org/10.9767/bcrec.20029

1. Introduction

With the development of technology and increasing life pursuit from the huge global population, wastewater especially for organic pollution has become a grimmer problem. It is majorly emitted from textile, paper, printing, and dyeing, and due to its variety, a corresponding treatment can be sophisticated [1]. Photocatalytic treatment has aroused attention in recent years and is determined to be a promising treatment method applied in industrial organic pollutants treatment for wastewater, considering its high efficiency, sustainability, and low cost for the degradation of wastewater [2]. Several types of photocatalyst have been applied and examined to be feasible, such as cobalt oxide (Co_3O_4) [2], graphitic carbon nitride/titania (g-

---

* Corresponding Author.
Email: sinyuan.lai@xmu.edu.my (Sin Yuan Lai)
Authors of K. Kong and Z. Zhu contributed equally to the work.

C_3N_4/TiO_2) [3], and barium titanate ($BaTiO_3$) [3]. Despite several efficient photocatalysts tested to be available to degrade organic pollution, challenges still remain, such as low photocatalytic activity for g-C_3N_4/TiO_2 [4], unstable function in degradation process, complex and limited literature for synthesis [2]. Thus, it is more urgent to explore a photocatalyst with high stability, low-cost and simple synthesis, and high efficiency in practical degradation of organic pollutants.

Graphene is a two-dimensional (2D) crystal composed of sp^2 hybrid carbon atoms, which has the advantages of large surface area, fast electron migration rate and high chemical stability. In the photocatalytic process, it can improve the adsorption of pollutants on the catalyst surface, accelerate the transfer of photogenerated electrons, and inhibit the combination of photogenerated electrons and holes. Graphene resembles a honeycomb crystal-like sheet with carbon atoms tightly bonded, and the thickness of each atom is about 0.335 nm [5]. The thermal and electrical conductivity of graphene is explored to be about 5300 W/mK and 106 S/m, making it possible to be introduced in many materials as a composite that can enhance their properties. It is a stronger material [6], where it can strengthen the stiffness of graphene-based material. It also shows great optical function and property with optical transmittance of around 97.7% [7], making it an ideal electronic sink, or electron-transfer bridge and a 2D support matrix for photocatalyst carrier [8].

Nowadays, applications of 2D graphene in different parts of technology, such as biomedicals, sensing, and electronic equipment, have been highlighted, but a concise review of 2D graphene-based photocatalyst utilized to process organic wastewater remains limited. Therefore, this article mainly describes currently developed 2D graphene doped with various types of materials, including titanium oxide (TiO_2), zinc oxide (ZnO), cadmium sulfide (CdS), and bismuth oxychloride (BiOCl). Additionally, the properties of TiO_2-, ZnO-, CdS-, and BiOCl-graphene based photocatalysts in degradation of organic pollutants, are described. Various types of synthesis method are also elucidated, in conjunction with their pros and cons, are analyzed and compared.

2. Graphene and Its Derivatives as Photocatalysts

Graphene possesses a lot of unique properties, like large surface area, great thermal conductivity, and great carrier mobility, which allows it to become an excellent hybrid counterpart of another photocatalyst [9]. It has been widely used in various applications, including transportation, medicine, electronics, etc., due to its low cost of production and versatility. One of the most important advantages is the unique electronic properties that come with its 2D crystal lattice structure. However, based on Figure 1(a), conduction band and valence band contact each other at the Dirac point, showing zero-band conducting capability (zero bandgap) [10]. This is crucial in designing a more efficient graphene-based photocatalyst by chemical modification [11].

Interestingly, graphene can transform from semimetal to semiconductor if it is covered with oxygen functionalities. This helps to fine-tune the optical and electronic properties of graphene to act as a standalone, metal-free photocatalyst. While introducing oxygen func-

(a)

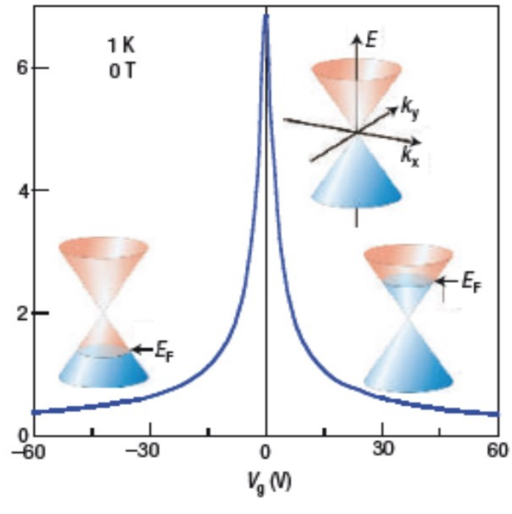

(b)

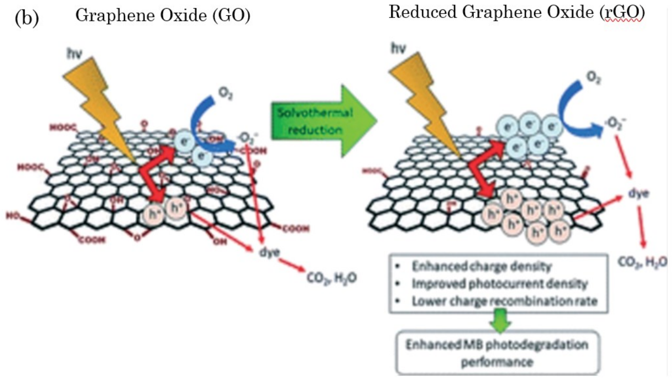

Figure 1(a). Ambipolar electric field effect in single-layer graphene, whereby the conduction and valence bands interact at the Dirac point without an external field [10]. (b) Mechanisms of visible light-active GO and rGO in dye degradation [14].

tionalities, the band gap is increased and the minimum valence band changes from π orbital of graphene to 2p orbital of oxygen [12], forming graphene oxide (GO). The derivatives of graphene, not only GO, but also reduced graphene oxide (rGO), are capable of photocatalytic activities [13] with a band gap ranging from 2.4 to 4.3 eV. Both GO and rGO could decelerate the photogenerated electron-hole recombination by accelerate the photogenerated electrons transmission speed. They demonstrate mechanisms of visible light-responsive dye photodegradation owing to their relatively narrow bandgap, as illustrated in Figure 1(b) [14]. In a recent study, rGO has shown its photodegradation efficiency towards methylene blue (MB) due to its high density of charge carrier and photocurrent density, as well as great charge separation [15]. Figure 2 describes the general merits offered by graphene-based photocatalysts. Additionally, both GO and rGO advocate good agreement with pseudo-first order kinetic plot [16,17]. The photodegradation of organic wastes using graphene-based photocatalysts also fit into the pseudo-first order reaction [18–21].

Despite of exhibiting photodegradation ability, GO and rGO are yet inferior compared to other graphene-based composites [14,19,22]. For instance, P25 degraded 76.7% MB, rGO degraded 71.7% MB, and TiO_2/rGO degraded 96.8% at 120 min. Despite of being low catalytic performance, rGO showed a better performance after incorporated with titanium isopropoxide as the precursor of TiO_2 [19]. It might due to rGO alone has less catalytic reactive sites, thus coupling with TiO_2 could improve this limitation.

3. Preparation Methods of Graphene-based Photocatalyst

3.1 Hydrothermal Technique

Hydrothermal technique is an effective way to enhance the structure, morphology, and photocatalytic efficiency of graphene-based photocatalyst [23]. It is a solution reaction-based method that is characteristically significant for a high yield and low-cost method. In order to control the size and morphology of the photocatalysts, high pressure or low pressure can be utilized according to the vapor pressure of the main compartment in the reaction [24]. When high pressure is utilized, low-boiling point solvents can be chosen. This is beneficial since the cost of high boiling point solvent such as dimethyl sulfoxide (DMSO) is generally more expensive and possesses toxicity. For high-temperature operation, hydrothermal synthesis is capable of controlling the quality of the desired nanocrystal [25]. However, one of the biggest downsides of the hydrothermal technique is the inability to monitor material crystal growth since the operation is conducted in the autoclave. Moreover, the equipment cost is considered high, which is worth considering before utilizing it [26–29]. The paragraph below shows the examples of producing graphene-based photocatalyst using the hydrothermal technique.

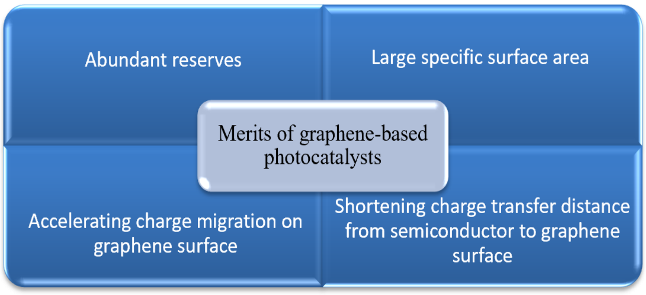

Figure 2. The advantages of graphene-based photocatalysts

In general, NaOH is deemed as one of the most popular solvents among material preparation technique including hydrothermal synthesis. For one of the examples of hydrothermal synthesis, 10 mL of g-C_3N_4 is paired with a 10 mL mixture of graphene oxide (GO) and to be followed by the suspension treated under ultrasonication for 30 min. In this instance, GO nanosheet acts as a surfactant to dissolve the g-C_3N_4 which ultimately improves the GO/g-C_3N_4 photocatalyst [30]. Furthermore, TiO_2/RGO nanocomposite can be prepared by the one-step hydrothermal process according to Hu *et al.* [31]. On the other hand, one-step hydrothermal synthesis can also produce TiO_2/G photocatalyst as the reduction of graphene oxide and the hydrolysis of $TiCl_4$ are conducted at the same time. In this case, $TiCl_4$ is used to produce TiO_2 nanoparticles [25].

3.2 Solvothermal Process

The solvothermal process prepares graphene-based photocatalysts with several morphological structures. It is similar to the hydrothermal method, but using organic matter or non-aqueous medium as solvent instead of water [32]. The reaction is usually conducted in a closed system like an autoclave. In this case, the autoclave is filled with a solution that undergoes reaction in a high temperature and pressure situation. When compared with the hydrothermal technique, solvothermal process generally has better controllability on the size distribution, shape, and crystallinity of the desired nanomaterials. This is because of the viscosity and polarity that is present in the solvent used in the process and the higher temperature [25,26]. Similar to hydrothermal technique, since the process is conducted in an autoclave, the inability to monitor the materialization of the process is its main issue. Lastly, this method has certain risks related to high operation conditions and careful operation is needed to avoid any incident, and precursor is needed in this method.

In the fabrication process, GO is mixed with g-C_3N_4 and 1-methyl-2-pyrrolidinone, leading to sonication for 2 h to get brown color. Afterward, CH_3COOH and acetyl trimethyl ammonium bromide solution is mixed with the previous solution. Next, Na_2MoO_4 and thiourea are added and stirred rapidly. Ultimately, the solution was injected into a Teflon-lined autoclave and stored at 200 °C for 24 h [33].

One-step solvothermal process was utilized in Wang's study to synthesize graphene/carbon nanotubes/TiO_2 nanocomposites. Tetrabutyl titanate was used as a TiO_2 precursor to mix with graphene oxide and multi-wall carbon nanotubes in 2-propanol. In terms of photocatalytic activity of the nanocomposites, it is mainly dependent on the content of carbon nanotubes, proving 5 wt.% is the optimum value. It helps to improve the photocatalytic efficiency by improving the OH^- formation, which is the main component of degrading organic pollutants [34].

3.3 Co-precipitation Process

Coprecipitation is becoming more essential as a method of distributing ingredients and precursors utilized in a reaction to make a necessary substance. Coprecipitation aims to prepare multi-component materials by forming intermediate precipitates, mainly hydrous oxides or oxalates, that form an intimate mixing of components during precipitation and maintain chemical homogeneity after calcination [34]. Co-precipitation process has been widely used for the production of GO/semiconductors-based photocatalysts [24]. It is recognized as a facile and economical method in terms of industrial-scale [36]. It is generally a method composed of simultaneous precipitation of a normal soluble component and a macro-component from the same solution by forming crystal, adsorption, or mechanical entrapment. In comparison to other synthesis techniques, the coprecipitation approach produces crystalline sizes in the tiny range, depending on the precipitant used during the reaction. Capping agents can also be used to modify the crystallinity and shape of the material produced using this process. The coprecipitation process, on the other hand, has a number of drawbacks, including the need for constant washing, drying, and calcination to create a pure phosphor phase.

For instance, GO was mixed with distilled water and sonicated before adding AgBr/g-C_3N_4 into polytetrafluoroethylene. Following that, distilled water was dispersed and the solution was sonicated. After heating at 180 °C for 6 h, the resulting material was repeatedly washed with ethanol and dried to get rGO/PCN/AgBr photocatalyst [37].

3.4 Sol-gel Method

Among the mentioned preparation methods, sol-gel method is the most complex method but has increasingly attracted attention in terms of preparing GO-supported semiconductors photocatalysts. It involves a transformation of the precursor to a sol that can eventually turn into a gel network structure [38]. In general, metal salts and alkoxides act as feedstock which undergoes a series of hydrolysis and polycondensation processes to form a colloid [24]. Doing so, has its upsides which are high purity and homogeneity in the final results, low operating conditions, low cost, and a simple manufacturing process. One of its biggest advantages is that, unlike hydrothermal and solvothermal methods, elevated temperatures and pressure are not essential.

According to Xu *et al.* [39], rGO/TiO_2 can be synthesized through a sol-gel method which leads to photocatalytic degradation of organic pollutants under visible light irradiation. One-step sol-gel method was utilized to synthesize TiO_2/GO nanocomposites with varying GO contents [40]. Furthermore, CdS-G-TiO_2 nanocomposites were prepared by sol-gel process whereby titanium oxysulfate precursor was used. In this particular case, due to bandgap narrowing and increased visible light absorption, CdS boosted the photocatalytic degradation of methylene blue under visible light illumination [41]. Please refer to a comparative table (Table 1) for each of the synthesis method.

4. Graphene-based TiO_2 Photocatalysts

4.1 TiO_2-Graphene

To date, graphene-TiO_2 composite photocatalysts have been getting increased attention due to their high performance. Graphene-modified TiO_2-composite photocatalysts possess several advantages, such as low toxicity, high reaction activity, and high stability [42]. This photocatalyst has been widely used in various applications, namely photocatalytic water decontamination, water disinfection, photocatalytic air pollution control, and so forth [42–45]. Nevertheless, two downsides of graphene-TiO_2 composite photocatalysts are low response rate of visible light and limited widespread application due to the high recombination rate of electron-hole pairs [42].

TiO_2 is widely known as an effective photocatalyst under UV light illumination. The photo-induced electrons and holes transfer to the surface of TiO_2 after being excited on the conduction band and valence band, respectively at wavelength less than 390 nm [42]. Next, the electrons react with oxygen to produce a superoxide anion (O_2^-). It is important to note that the oxygen is dissolved in the aqueous solution, while the holes react with the hydroxyl to obtain hydroxyl free radical (OH•) [42]. Eventually, the anion and the hydroxyl free radical become the factors that are responsible for decomposing the pollutant molecule into carbon dioxide and H_2O since they are strong oxidizing agents. Since the presence of these oxidizing radicals determines the performance of the photocatalytic activity, the recombination rate of the electron-hole pairs needs to be put into consideration to improve the performance. In this case, an electron tank can be utilized to hinder the recombination rate of electrons and holes in TiO_2. In graphene-TiO_2 composite photocatalyst, graphene acts as an electron tank since it is competent as compared to other carbon allotropes due to its high electron mobility [42,46]. Figure 3 illustrates the details working mechanism of graphene-TiO_2 composite photocatalyst and pure TiO_2.

TiO_2 shows limited photocatalytic activity with low response rate under visible light irradiation [47]. To resolve the issue, zero bandgap structure of graphene makes it a sensitive sensitizer to improve this situation. Under visible light irradiation, electrons are excited on

Table 1. Comparative table of each synthesis method

Synthesis method	Advantages	Disadvantages	References
Hydrothermal technique	High yield Low-cost process Greatly alter size and morphology Produce large crystal with high quality	Inability to monitor material crystal growth High equipment costs	[15,116]
Solvothermal process	Uses organic matter Better controllability on the size distribution, shape and crystallinity Readily obtained single crestal	Inability to monitor material crystal growth High operation condition and careful operation is needed Require soluble precursors	[15,117]
Co-precipitation process	High yield High product purity Easy reproducibility Capping agent modify the crystallinity and shape	Produce toxicant the need for constant washing, drying, and calcination Require monitoring breakthrough	[15,35]
Sol-gel method	High purity and homogeneity Low operating condition Simple, economical and efficient method	Long processing time Organic solutions used can be toxic	[15,116]

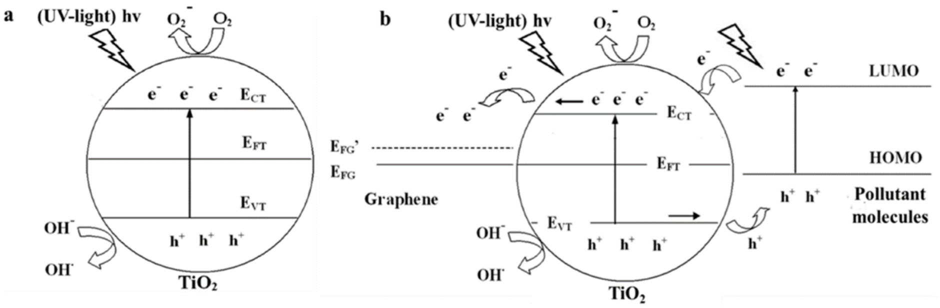

Figure 3. Illustration of the working mechanism of graphene-TiO_2 photocatalyst under UV light [42,114]

the Fermi level of graphene. To inject the electrons into the conduction band of TiO_2, the Schottky barrier needs to be overcome. In the case of graphene, graphene-TiO_2 composite possesses no significant band bending since the size of graphene is tinier than the size of the space-charged region. The excited electrons in graphene are injected into TiO_2 by quantum tunneling and thermionic emission to overcome the thin Schottky barrier. The mechanism of graphene-TiO_2 photocatalyst under visible light irradiation is shown in Figure 4.

To curb the fast electron-hole pairs recombination rate, heterojunction properties have been widely proven as a capable property of photocatalysts to promote spatial separation of photoinduced electron-hole pairs which ultimately improves the overall photocatalytic activity [48,49]. For instance, the graphene-wrapped TiO_2 hybrid possesses Schottky heterojunctions that are fabricated through direct wrapping of rGO on the surface of TiO_2 [49,50]. The formation of Schottky heterojunction in graphene wrapped TiO_2 hybrid is believed to have a positive impact on photocatalytic activity by decreasing the semiconductor to graphene barrier and promoting the transfer of electrons from the conduction band of TiO_2 to the graphene surface. Generally, metallic graphene is utilized to compose the Schottky heterojunction and it usually acts as a co-catalyst. This leads to the excellent synergistic effects of graphene to capture photoinduced electrons which enhances the photocatalytic degradation activity [50]. To further optimize the Schottky heterojunction, the conductivity of the graphene could be improved to reduce the defect sites or by utilizing highly conductive materials such as polyaniline [51,52].

It's worth noting that graphene has high stability with all these strong oxidizing radicals (O_2^{-} and OH•), as seen by the high photocatalytic efficiency after cycle use. When compared to the first performance of a photodegradation process, the breakdown rate of several contaminants maintains more than 90% after repeated use [53,54]. Furthermore, the shape of graphene in graphene-TiO_2 photocatalysts shows no significant change after recycling use. In Tang's works [42], the performance of graphene-TiO_2 remains about 95% after 20 successive cycles. It is because graphene is inert towards oxidizing radicals, and hence, resulting graphene-TiO_2's stability during photocatalytic reaction.

TiO_2 can be identified in three different forms which includes anatase, rutile and brookite as shown in Figure 5. Anatase and rutile exist in tetragonal structure, whereas the anatase structure possesses no corner sharing. On the other hand, brookite exists in orthorhombic structure with no corners and edges

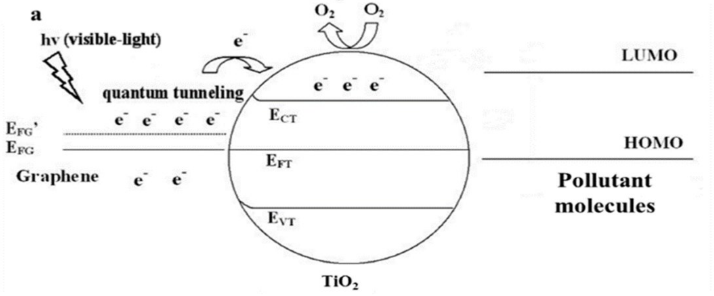

Figure 4. Illustration of the working mechanism of graphene-TiO_2 photocatalyst under visible light [114]

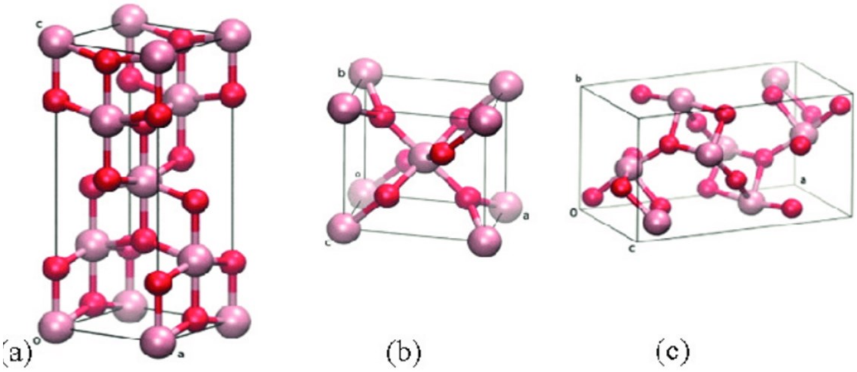

Figure 5. Structures of TiO_2: a) anatase, (b) rutile, (c) brookite [115]

connection. In general, rutile is considered a stable form while anatase and brookite can be transformed into rutile when heated. Owing to unfavorable electron-hole recombination limits the effectiveness of the photocatalytic process, linking two different forms of semiconductor materials could help to improve electron-hole charge separation and therefore prevent rapid recombination of energized electrons with electron vacancies in the valence band [55]. The creation of TiO_2 nanoparticles with varied morphologies can be achieved by simple control of the reaction environment combined with the stabilizing impact of the added substrates. The presence of {001}, {101}, and {100} facets affect their photocatalytic activity. In terms of anatase TiO_2, {001} facets are generally known as the more reactive alternative due to its high surface free energy and abundant unsaturated coordinated atoms. Nevertheless, co-existing facets should also be considered since they can have synergistic effects in the separation of photogenerated electron-hole pairs, which can enhance the photocatalytic efficiency. For instance, {101} facets can provide large surface area of reduction sites, which contributes to collection of photo-generated electrons and prevent the recombination of electron-hole pairs [56].

In short, pairing graphene with TiO_2 allows graphene to act as electron tank due to its high electron mobility to hinder the recombination rate of the electron-hole pairs. Also, the stability of graphene has great contribution towards the efficiency of graphene-TiO_2 nanocomposite, which can be proven since the shape of graphene in graphene-TiO_2 photocatalysts shows no significant change after photodegradation. However, the production of cheap high-quality graphene at industrial scale remains a tremendous challenge as it hinders the efficiency of graphene-TiO_2-nanocomposite. In the following section, graphene oxide is discussed, since it is easier to be produced as compared to pristine graphene.

4.2 TiO_2/Graphene Oxide (TiO_2/GO)

To enhance the efficiency of TiO_2 photocatalytic activity, carbon-based materials, like graphene, has been proven to be effective since they have wide coverage of visible light and minimizing electron-hole recombination [56]. However, as graphene is expensive and relatively difficult to produce, graphene oxide (GO) was considered an inexpensive alternative. It is a single-atomic layered material produced by the powerful oxidation of graphite, a cheap and abundant material. GO is an oxidized form of graphene that has been impregnated with oxygen-containing groups. It is considerably simple to process because its high dissolution rate in water.

Many studies have been conducted on TiO_2/GO composites. This material is discovered to be superior to bare TiO_2. Natural properties of GO, such as large theoretical specific surface area, high adsorptive capacity, and electron-hole separation effectivity, are among the qualities that aid TiO_2/GO composite photocatalytic performance significantly [58]. For instance, TiO_2/GO nanocomposite synthesized using a one-step hydrothermal method exhibits four major improvements, including extended light absorption range, more effective charge transfer, higher adsorption capacity, and 70–85% photocatalyzed dye decomposition in less than an hour [59].

One of the approaches that can be utilized to enhance the optical absorption of TiO_2 into the visible light region is doping. Doping TiO_2 with Lanthanide elements increases its photocatalytic activity [60,61]. Lanthanides are ideal elements for modifying the crystal structure, electronic structure, optical properties, surface adsorption of TiO_2 and forming a series of novel promising photocatalysts due to their unique 4f electronic configuration and spectral characteristics. Lanthanides allow for a more in-depth investigation of the electronic structure which can improve TiO_2's photocatalytic activity [61]. In Mariam's works [62], photocatalytic activity of lanthanide doped TiO_2 nanocomposite paired with GO to form a new composite nanomaterial have been studied. In this case, Sm^{3+} and Eu^{3+} has been used to dope with TiO_2. The results show that increasing the lanthanide dopant ion concentration increased the photocatalytic degradation rate of MB until an optimum concentration was reached. However, further increment of the concentration of lanthanide metal ions as a dopant metal ion retarded the photodegradation rate of the dye solution.

To explain further, a dopant acts as a charge carrier separator to increase charge separation and improve the photocatalytic efficiency of the nanocomposite. However, at a higher metal concentration, the dopant can act as a charge recombination center, preventing the separation of photogenerated charge carriers and suppressing the generation of oxygen radicals, thus resulting in a decrease in the photocatalytic process [63]. As a result, controlling the dose of metal dopants in nanocomposites is an important factor in photocatalysis enhancement. On the other hand, the large specific surface area of GO and its oxygen-containing functional groups increased absorptivity and followed by pollutant degradability. The GO content acted as a photosensitizer and electron scavenger, reducing photogenerated electron-hole pair recombination and thus increasing absorbance in the visible region, resulting in high photocatalytic activity [62].

Apart from that, the doping of TiO_2 with nonmetal atoms, such as nitrogen, has received a lot of attention, and it can extend TiO_2 absorption to the visible region. Single element doping, such as N and S, was investigated to improve TiO_2 photocatalytic efficiency because the resulting oxynitrides and oxysulphides absorb visible light to some extent [64,65]. From Shang's works [66], S-, N-doped TiO_2/GO composites was investigated to determine the effect of doping on TiO_2. The reports have shown that S-, N-doped TiO_2/GO is a better photocatalyst than undoped photocatalyst since S-, N-doped TiO_2/GO expand the wavelength response range into the visible region and increase the number of photo-generated electrons and holes to participate in the photocatalytic reaction. Hence, when compared to TiO_2/GO, S and N improve photocatalytic activity by increasing the number of photo-generated holes and electrons that take part in the photocatalytic activity.

Briefly, GO is an inexpensive alternative to graphene and is simple to process because its solubility in water (polar dissolves polar). GO acts as a photosensitizer and an electron scavenger, reducing photogenerated electron-hole pair recombination, and thus increasing absorbance in the visible region, resulting in high photocatalytic activity. Doping engineering has also been discussed in terms of enhancing the optical absorption of TiO_2 into the visible light region. Doping agent like Lanthanides and nitrogen can act as a charge carrier separator below an optimum dopant metal ion concentration, increase charge separation, and improve the photocatalytic efficiency of the nanocomposite. Another fabrication of graphene-TiO_2 photocatalyst is pairing TiO_2 with reduced graphene oxide (rGO). Due to the chemical and structural differences, GO and rGO show different mechanical, electrical, and chemical properties. In the next section, TiO_2/rGO will be discussed.

4.3 TiO_2/Reduced Graphene Oxide (TiO_2/rGO)

GO and rGO have each proven to be valuable graphene derivatives. However, they differ significantly in terms of structural and chemical properties. The biggest distinction between GO and rGO is the C/O ratio in their structure. While the C/O ratio in GO structures is very low, it is considerably higher in rGO structures, approaching almost negligible oxygen content. The remaining differences between GO and rGO materials are primarily due to this difference in C/O ratios. The electrical conductivity of these two materials is thought to be the most notable change. While GO is insulating or semi-conducting, rGO has a high electrical conductivity. In terms of comparing GO and rGO pairing with TiO_2, rGO improves the shuttling and possible catalytic position [67]. Besides, rGO is more stable than GO and has similar properties as graphene [68].

In report published by Yu *et al.* [67], the team has investigated the photocatalytic activity of an Ag/TiO_2/rGO nanocomposite by measuring the photocatalytic degradation of MB dye under visible light using a Xenon (Xe) lamp. Figure 6 shows the comparison between three separate systems, i.e. bare TiO_2, TiO_2/rGO and Ag/TiO_2/rGO. The photocatalytic efficiency of two nanocomposites (TiO_2/rGO and Ag/TiO_2/rGO) is higher than the bare TiO_2. It could be deduced that the rGO has better adsorptivity with MB owing to its larger surface area. On the other hand, TiO_2 nanoparticles prevented graphene sheets from aggregating. Also, as mentioned in the previous section, the existence of graphene can prevent the recombination of electron-hole with the electron injection into graphene. Moreover, the addition of Ag doping has improved the photocatalytic activity over TiO_2/rGO due to the effect of the existence of Schottky barriers at the interface of Ag and TiO_2. It helps to serve as an electron trap to inhibit electron-hole recombination.

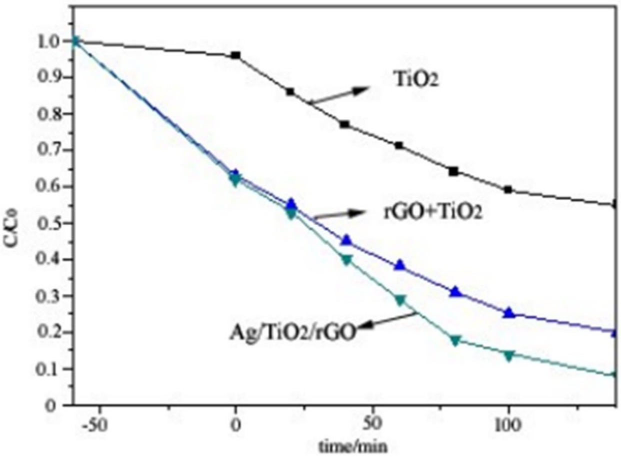

Figure 6. Photocatalytic degradation of methylene blue for bare TiO_2, TiO_2/rGO and Ag/TiO_2/rGO [66]

Beside from Ag, Fe is also an excellent doping agent since it could improve the photocatalytic activity by increasing the number of active sites and narrowing the band gap of TiO_2 [69]. Moreover, the similarity of the redox potentials of Fe^{2+}/Fe^{3+} and Ti^{3+}/Ti^{4+} extends its application, which expands its light absorption to the visible spectrum, allowing sunlight to be used as a source of energy [70]. According to Ali report [68], Fe-TiO_2/rGO exhibit a high stable photocatalytic activity for the decontamination of Rhodamine B under solar irradiation.

Doping Ce on TiO_2/rGO composite film inhibited the TiO_2 anatase-rutile phase transformation [71]. In this case, Ce atoms could act as a dispersion oxide, preventing photoinduced electron-hole pair recombination. Furthermore, the absorbance of Ce doped TiO_2/rGO nanocomposite films changed from UV to visible region. Under solar simulator irradiation, the Ce doped TiO_2/rGO composite film demonstrated superior photoelectrochemical performance to TiO_2/rGO composite and pristine TiO_2. The main reason could be the content of Ce, which could act as an electron acceptor to reduce recombination loss and facilitate better transportation of photoinduced charge carriers [72]. Last but not least, there were reports investigating combining TiO_2 and ZnO pairing with each other. It was found out to be an effective solution as it could potentially prevent the recombination process and prolong the lifetime of electron-hole pairs [73].

To recap, rGO is by far the most essential choice to pair with TiO_2. Graphene and GO possess determining downsides that makes it inefficient to pair with TiO_2. Firstly, production of cheap high-quality graphene at industrial scale remains a tremendous challenge. Many of the top-down techniques like chemical vapor deposition, silicon evaporation and epitaxial growth are limited to liquid medium for graphene stabilization, resulting in inefficient solvent removal, low graphene yields and the existence of defect [74–76]. On the other end of the spectrum, bottom-up techniques require expensive equipment and high-quality graphene that is grown inadequately in the high temperature circumstances.

In the case of Gin, the synthesis process of GO, strong oxidants allow GO to present significant amount of defects in its crystalline network. As a result, GO's conductive properties are far inferior to those of graphene, though its optical and mechanical O, properties suffer less. Fortunately, supplemental reductive exfoliation treatments that convert GO to rGO can restore graphene-like properties to GO [77,78]. rGO is currently a very decent solution between graphene and GO. This is due not only to rGO's graphene-like properties, such as fairly decent conductivity, but also to rGO's ease of preparation in desired quantities from inexpensive GO. Hence, rGO is by far the most essential choice to pair with TiO_2. Table 2 shows a summary of organic pollutants degradation over graphene-based TiO_2.

Table 2. Summary of organic pollutants degradation over graphene-based TiO_2

Photocatalysts	Dopants/ Co-catalysts	Pollutants	Light Source	Degradation, %	Time, min	Cycle	Cycle effect	Ref.
Bi/SnO_2/TiO_2/G	Bi/SnO_2	PCP	Sunlight through sunlight collector	84	120	5	68% in last cycle	[118]
TiO_2/G	-	Methyl orange	300 W Hg lamp	85	60	-	-	[119]
Ln(III)-TiO_2/GO	Ln(III)	Methylene Blue	3 mW.cm^{-2} UV light	-	90	-	-	[69]
Ag-TiO_2/GO	Ag	Phenol	6 W visible light	60	180	-	-	[120]
N-TiO_2/GO	N	Methylene Blue	120W UV lamp	86.5	60	Hard to recycle	-	[121]
CuO-TiO_2/rGO	CuO	Methyl Orange	40 (kHz) UV light	>98	90	5	Consistently more than 90%	[122]
Ag-TiO_2/rGO	Ag	Methylene Blue	150W Xe lamp	90	140	-	-	[67]
Ag-TiO_2/rGO	Ag	Formaldehyde	300W UV lamp	77.08	120	-	-	[123]
ZnO-TiO_2/rGO	ZnO	Methylene Blue	11W UV light	99.84	60	5	Still greater than 97%	[124]
Ce-TiO_2/rGO	Ce	Methylene Blue	250W Mercury-vapor lamp	100	90	3	Negligible decrease of degradation efficiency	[125]

5. Other Graphene-based Photocatalysts

5.1 ZnO/Graphene-based Nanocomposites

Zinc Oxide (ZnO) is deemed as a semiconductor with hexagonal wurtzite crystal structure as its most common and stable form. It possesses properties, which are good electrical and thermal conductivity, high-temperature stability, and reasonable cost [79,80]. With the versatility in morphology, dimensionality, size, and shape of ZnO, it possesses various variations of physical and chemical properties. Hence, the size of the morphology of ZnO morphology can enhance photocatalytic activity [81,82]. Also, it possesses prominent properties like good carrier migration efficiency and large surface area which would influence the photocatalytic activity. Similar to many semiconductors, it has drawbacks like high recombination rate of charge carrier and instability in extreme pH conditions which hinders the effect of commercial application in photocatalytic activity [79]. When coupling graphene with ZnO, graphene reduces the bandgap energy of ZnO which enables the absorption efficiency of visible light. As mentioned in previous graphene-based photocatalysts, it hinders the recombination rate of charge carriers which ultimately improves the photocatalytic efficiency.

The sol-gel method has been utilized extensively to synthesize various transition metal oxides. It is a well-known wet-chemical method to form ZnO-graphene nanocomposites by combining ZnO nanoparticles onto the surface of GO sheets. This produces a nanostructure with a high surface area, which enhances the adsorption capability to improve the photocatalytic efficiency [83]. Moreover, different shapes and sizes of nanocomposites can be synthesized and the process is operated at a low temperature and possesses high controllability on the chemical composition [79]. With different morphology, the properties can vastly defer from each other since the morphology can affect photocatalytic activities.

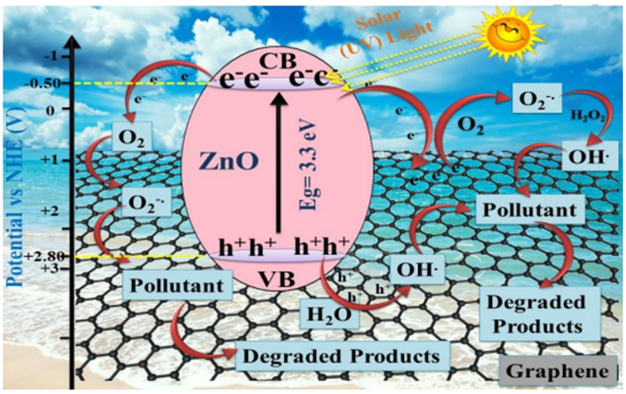

Figure 7. Illustration of the working mechanism of photodegradation process of ZnO/graphene nanocomposite photocatalyst [84]

The illustrated mechanism of photodegradation of pollutants using ZnO/graphene nanocomposite is shown in Figure 7. First of all, the electrons are excited under suitable energy sources, such as solar light, reacts with oxygen to produce a superoxide anion. In the meantime, the holes react with H_2O to form hydroxyl radicals. Next, the degradation of the pollutant happens on the surface of the ZnO-graphene nanocomposite. In this case, graphene hinders the recombination of holes and charge carriers onto the surface of ZnO, which ultimately improves the efficiency of the photodegradation process [84].

Moving over to the heterojunction properties, semiconductor heterojunction can be divided into Type I, Type II, and Type III. However, Type II heterojunction is the only one that can improve the charge separation and photocatalytic activity. Among the Type II heterojunctions, ZnO-graphene nanocomposites possess p-n heterojunction which increases the number of electrons that could be excited by higher energy irradiation [85]. The p-n heterojunctions consist of p-type graphene and n-type ZnO semiconductor. The p-n heterojunction could hinder the rapid recombination of photoinduced electron-hole pairs, ultimately improving the photocatalytic activity [86].

In terms of the morphology of ZnO, the morphology is highly affected by the synthesis method which can be categorized into spheres, rods, flowers, flakes, etc. [87]. Following that, photocatalytic efficiency is dependent on morphology. SEM can be utilized in the characterization of photocatalysts. By incorporating graphene into ZnO nanoparticles, the nanocomposite possess several upsides, for instances: i) increase in crystallinity; ii) more intimate contact between ZnO and graphene surface; iii) excellent graphitic sp^2 C=C crystal structure of graphene nanosheet; iv) increased surface area; v) enhancement of absorption of light which all results in a positive impact on the photocatalytic activity of the nanocomposite. Lastly, incorporation of graphene nanosheet to ZnO, easy transportation of photoinduced electrons allows better separation of charge carriers which ultimately increases the photocatalytic efficiency. These produce a conclusion that graphene-modified ZnO photocatalyst is definitely a greater system over pristine ZnO [87].

5.2 CdS/Graphene-based Nanomaterials

CdS is a semiconductor material possessing a band gap of 2.4 eV and high absorption, which allows it to be a viable visible light photocatalyst when compared to others [88,89]. According to Cao *et al.* [90], CdS shows efficient photocatalytic degradation when studying tetracycline degradation using CdS/nitrogen/carbon composite [91]. However, one huge downside of CdS is its high susceptible to corrosion by light which hinders the sustainability of this photocatalyst [92]. Hence, the strategy of incorporating CdS with rGO has been studied to enhance its photocatalytic activity to further improve the efficiency. As mentioned in previous sections, graphene possesses great properties, such as effective adsorption properties and high electron mobility with a great surface area which allows the pairing of both substances to have a positive impact on the photocatalytic degradation process.

Solvothermal has been deemed as one of the leading methods to fabricate CdS-based photocatalysts lately. As mentioned in the previous section, it possesses advantages like high controllability of size, shape, and phase of CdS particles by manipulating related conditions like temperature, precursor concentration, and reaction time [93]. Moreover, the solvothermal method beats hydrothermal method by higher chemical reactivity, dispersion, and improved dissolution of reactants [94]. When GO has paired with CdS nanoparticles, it can receive and transport electrons from an excited semiconductor efficiently, which is advantageous for charge suppression, recombination rate, and lastly, to improve the interfacial charge for photocatalytic activity [95].

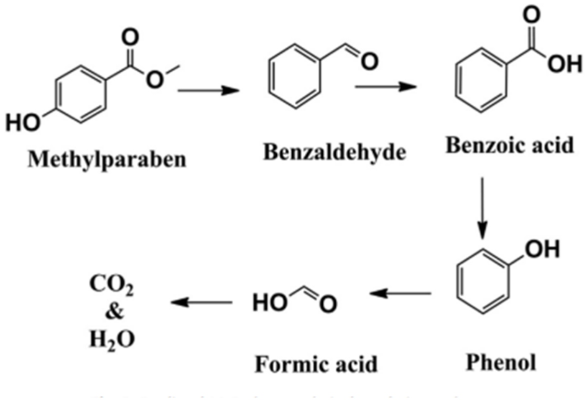

Figure 8. Photodegradation pathway of methylparaben using CdS/rGO nanocomposite [89]

As mentioned in the previous paragraph, CdS has a band gap of 2.4 eV whereas the valence and conduction bands are determined to be 1.45 and -0.95eV [96]. When CdS is irradiated, electrons are photogenerated and eventually transferred to rGO due to CdS being more negative than the work function of rGO [89]. Then, the electrons react with the oxygen to produce superoxide anion and hydroxyl radicals which ultimately contribute to the degradation of the organic pollutants. In the process of transferring electrons, the charge separation is promoted which hinders the recombination rate and the hydroxyl group at the rGO surface hinders the corrosion of CdS caused by light. The photodegradation pathway of methylparaben using CdS/rGO nanocomposite is shown in Figure 8. Based on Mohan *et al.* [89], recyclability and stability of CdS/rGO nanocomposite was reviewed whereas it can degrade 100% of methylparaben for 9 cycles, indicating that it is an efficient photocatalyst environmentally and economically.

SEM and TEM are used to determine the surface morphological features of the pristine nanoparticles and CdS/rGO nanocomposite. First of all, spherical CdS nanoparticles have been evenly distributed all over the surface of rGO. The twisted nano-sheets of rGO are clearly and firmly decorated with CdS nanospheres. Hence, there is a strong interaction between two nanomaterials. The rGO sheets are obviously curled and wavy, with an uneven surface. The CdS nanoparticles, on the other hand, have a smaller diameter. Due to their round shape, particles have a lower aggregation affinity. This enables them to possess a greater surface area. The specific surface area acquired by the nanocomposite material was significantly greater than that of pristine CdS nanoparticles [97].

To determine the electric properties of Cds/rGO nanocomposite, Electrochemical Impedance Spectroscopy (EIS) Nyquist plots can be utilized to assess the related photo-response phenomenon with the influence of rGO on the CdS nanoparticles. In Mohan's research, the intensity of arc of rGO modified CdS nanoparticles is clearly lower than pristine CdS, resulting in the facilitation of interfacial charge transfer by rGO [98]. This allows rGO to be a great electron acceptor and mediator, resulting in a longer lifetime of excited electrons which ultimately hinder the recombination of electron-hole pairs [89,99]. Hence, photocatalytic activity can be improved.

5.3 BiOCl/Graphene-based Nanohybrids

Bismuth has been one of the more promising photocatalysts to date considering its good stability, reactivity, and light responsiveness [100–102]. Relevant state-of-the-art bismuth-based materials have been reviewed, such as barium potassium bismuth oxide [103], bismuth-based composite oxides [103], bismuth ferrite nanoparticles [105], bismuth oxyhalides [106], and more which excel in various types of photocatalytic application [107]. Hence, bismuth-based compounds are promising photocatalysts that possess high reactivity towards visible light which enables the pairing of bismuth and graphene as a composite photocatalyst. Pristine bismuth photocatalyst offers advantages like high stability, reusability, high photoactivity, and environmentally friendly as compared to other alternatives [102]. However, a few downsides, for examples, high recombination rate, slow transportation of charge carrier, and low visible light absorption hinder the performance of the pristine catalyst. Hence, graphene-modified bismuth photocatalyst to improve the performance has been reviewed [102].

To synthesize the bismuth-graphene-based nanohybrid, hydrothermal and solvothermal methods have been utilized extensively utilized due to the nature of high temperature and high pressure. Highly crystalline nanohybrid can be synthesized while GO was reduced using a one-pot hydrothermal and solvothermal method [102]. The morphology of the photocatalyst has been focused on extensively because the photocatalytic efficiency is not only dependent on the chemical phase but also on its size and shape. Hence, the hydrothermal method has been deemed as one of the most effective ways to synthesize this photocatalyst since it can effectively control the size and shape of the photocatalyst [102,108].

In this case, the studied bismuth-graphene nanohybrids are BiOCl/rGO photocatalyst. The photocatalyst operates under the effect of LED irradiation and the sample pollutant is set to be Rhodamine B. Upon the direct irradiation of the white LED of the BiOCl/rGO photocatalyst with RhB, an electron is generated upon the excitement of RhB. It is important to note that the RhB is in the singlet excited state. The specific electrons are then injected into the conduction band of BiOCl which is similar to TiO_2-graphene photocatalyst while the valence band remains intact. Then, the superoxide anion is produced through a series of oxidation and reduction reactions after the electrons are transferred to rGO and react with adsorbed oxygen molecules [109]. Eventually, RhB is degraded and decomposed. To conclude, RhB is utilized in inducing the activation of the photocatalyst and producing a superoxide anion. Also, the inclusion of rGO has improved the photocatalytic performance of the pristine photocatalyst by inducing the transportation of electrons to react with oxygen. The illustrated working mechanism of RhB degradation with BiOCl/rGO photocatalysts is shown in Figure 9.

To determine the morphology of BiOCl/GO nanocomposite, SEM, TEM, and EDX spectra can be utilized (Figure 10). BiOCl itself exhibits a flower-like morphology with a smooth surface with hierarchical structures. Graphene oxide exhibits sheet-like structures and is dispersed as well as interact with BiOCl on the contact interface. With continuous irradiation, the rGO exhibits a flower-like morphology with a looser morphology. In SEM images, these photocatalysts show a flower-like micron size particle. However, BiOCl/GO and BiOCl/rGO exhibit numerous and interconnect nanopores that match the result of the TEM image. The EDX spectrum has shown the composition of the photocatalyst [109]. BiOCl with flower-like structures has strong photocatalytic activity because the layered BiOCl structure can give enough space to polarize the associated atoms and orbitals, effectively separating the photogenerated electron–hole pairs and therefore increasing BiOCl's photocatalytic activity. Large specific surface area, on the other hand, has been shown to assist boost photocatalytic reaction sites and improve electron–hole separation

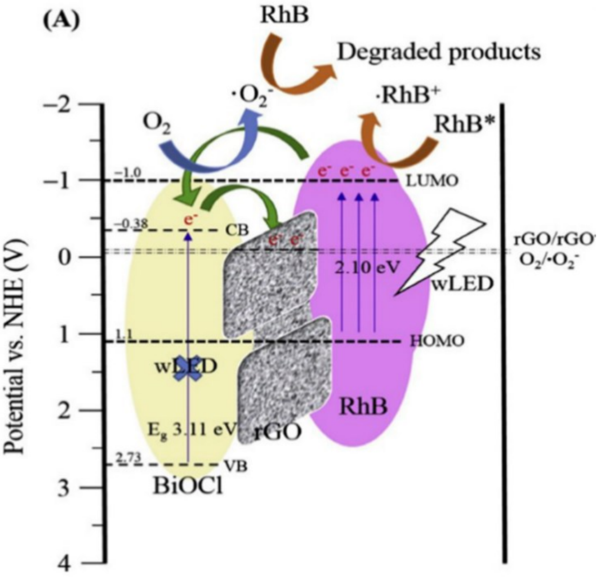

Figure 9. Illustration of the working mechanism of RhB degradation with BiOCl/rGO photocatalyst [102,109]

efficiency. Sun's group [110] has also utilized XRD to determine the stability of BIOCl and no significant change was observed for the phase and structure after the photocatalytic reaction which indicates it was stable throughout the photocatalytic reaction.

To further evaluate the modified bismuth photocatalyst with graphene oxide and reduced graphene oxide, RhB degradation under wLED irradiation was examined as covered above. In general, the RhB degradation is completed through a dye-sensitized reaction [111]. To emphasize, BiOCl/GO and BiOCl/rGO have exhibited better photocatalytic degradation efficiency than pristine BiOCl due to the ability of graphene to adsorb RhB effectively as well as its large surface area [112,113]. More active sites will be available to react with water and hydroxyl to create crucial oxidative hydroxyl radicals, as well as attach organic molecules for photodegradation. Ultimately, the BiOCl/rGO photocatalyst possesses the highest efficiency of 98.7% in 25 min. However, when it is prepared with a higher concentration of rGO, the ability to absorb visible light is hindered which eventually decreases the photodegradation efficiency.

In brief, BiOCl/rGO has shown promising photocatalytic degradation efficiency under wLED for organic pollutant degradation and excellent reusability, which can be reused for five runs before a significant drop in performance. Table 3 lists a summary of varieties of photocatalysts in organic waste degradation.

6. Conclusions and Future Outlooks

In this review, we summarize those four types of graphene-based semiconductors, viz. titania (TiO_2), zinc oxide (ZnO), cadmium sulfide (CdS), and bismuth oxychloride (BiOCl). Both TiO_2 and ZnO possess wide band gap and only respond to ultraviolet light (higher energy consumption). By coupling with graphene or its derivatives, i.e. graphene oxide (GO) and reduced graphene oxide (rGO), the band gap is narrowed and visible light responsive is viable. Despite being acquiring narrow band gap, CdS suffers from photo-corrosion. By functionalizing CdS onto graphene-based nanomaterials, charge suppression could be achieved effectively. BiOCl exhibits weak interfacial interaction with organic pollutants, however, the adsorptivity of the wastes onto BiOCl-graphene based photocatalyst is enhanced significantly. These materials possess high surface area, mechanical stability, chemical stability, high electron mobility, abundant surface-active site, and strong adsorbility. By combining all these strengths, a desired composite with better reducing and oxidizing ability, resulting better charge separation rate and more efficient light absorption could be attained. Hence, the discussed graphene-based photocatalysts are very

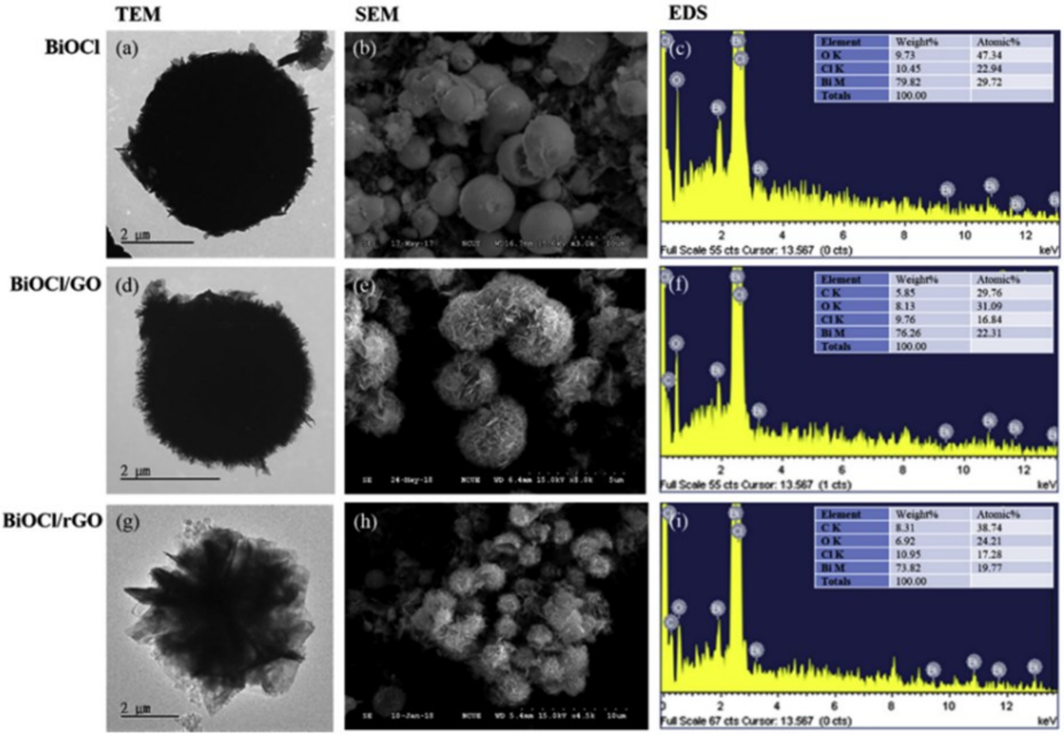

Element	Weight%	Atomic%
O K	9.73	47.34
Cl K	10.45	22.94
Bi M	79.82	29.72
Totals	100.00	

Element	Weight%	Atomic%
C K	5.85	29.76
O K	8.13	31.09
Cl K	9.76	16.84
Bi M	76.26	22.31
Totals	100.00	

Element	Weight%	Atomic%
C K	8.31	38.74
O K	6.92	24.21
Cl K	10.95	17.28
Bi M	73.82	19.77
Totals	100.00	

Figure 10. TEM and SEM images and EDX spectra of BiOCl and its modifications [109]

promising in photodegradation of organic hazardous materials, as evidenced by their exceptional performance of >80% efficiencies in less than 2 h. Certainly, this will further stimulate intense studies on the graphene-based photocatalysts in photodegradation of wastewater.

Undeniably, graphene and its derivatives have demonstrated their robust capability in treating environmental issues. Nevertheless, their full potential has yet to be exploited thoroughly. We believe that sophisticated designs could further harness the conversion of solar-to-chemical energy in various applications. Lastly, the collaboration between academia and industry in developing these materials could definitely hasten the realization of the renewable energy sector.

Acknowledgments

The work is supported by Xiamen University Malaysia Research Fund (grant number: XMUMRF/2019-C4/IENG/0019 and XMUMRF/2020-C5/IENG/0029) and Hengyuan International Sdn. Bhd. (grant number: EENG/0003).

CRediT Author Statement

Kelvert Kong: Methodology, Validation, Investigation, Writing - Original Draft, Visualization; Zhiying Zhu: Validation, Investigation, Writing - Original Draft; Mukhamad Nurhadi: Conceptualization, Writing - Review & Editing; Sumari Sumari: Conceptualization, Writing - Review & Editing; Siew Fan Wong: Writing - Review & Editing; Sin Yuan Lai: Conceptualization, Methodology, Validation, Investigation, Writing - Original Draft, Writing - Review & Editing, Visualization, Supervision, Project administration, Funding acquisition.

References

[1] Duan, X., Ren, D., Wang, S., Zhang, M., Sun, Y., Sun, S., Huo, Z., Zhang, N. (2023). Carbon materials in electrocatalytic oxidation systems for the treatment of organic pollutants in wastewater: A review. *Carbon Resources Conversion*, 6(4), 262–273. DOI: 10.1016/j.crcon.2023.03.006.

[2] Hu, Z., Hao, L., Quan, F., Guo, R. (2022). Recent developments of Co_3O_4-based materials as catalysts for the oxygen evolution reaction. *Catal. Sci. Technol.*, 12,436–461. DOI: 10.1039/D1CY01688A

[3] Masekela, D., Hintsho-Mbita, N.C., Sam, S., Yusuf, T.L., Mabuba, N. (2023). Application of $BaTiO_3$-based catalysts for piezocatalytic, photocatalytic and piezo-photocatalytic degradation of organic pollutants and bacterial disinfection in wastewater: A comprehensive review. *Arabian Journal of Chemistry,* 16. DOI: 10.1016/j.arabjc.2022.104473

[4] Sewnet, A., Abebe, M., Asaithambi, P., Alemayehu, E. (2022). Visible-Light-Driven g-C_3N_4/TiO_2 Based Heterojunction Nanocomposites for Photocatalytic Degradation of Organic Dyes in Wastewater: A Review. *Air, Soil and Water Research,* 15. DOI: 10.1177/117862212211172

Table 3. Summary of different varieties of photocatalyst

Photocatalyst	Reaction conditions			Light source	Organic pollutants	Degradation efficiency (%)	Reference
	Initial pollutant amount (mL)	Illumination time (min)	Pollutant concentration (mg/L)				
TiO_2/rGO	100	180	0.01	Visible light	Rhodamine B	84.6	[121,125]
	200	60	15	UV light	Methylene Blue	100	[121]
CuO-TiO_2/rGO	100	90	10	UV light	Methyl Orange	>98	[126]
BiOCl/rGO	250	310	4	Visible light	Rhodamine B	100	[127]
rGO/$Bi_2O_2CO_3$/	200	300	15	UV light	Sulfanilamide	82.7	[128]
BiOCl	40	120	20	UV light	Ciprofloxacin	90	[129]
ZnO/rGO	20	10	10	UV light	Methylene Blue	99	[130,131]
AgBr/ZnO/rGO	-	60	10	Visible light	Methyl Orange	0.2*	[131]
Cds/rGO	50	30	30	Visible light	Methylparaben	98	[88]

*: 0.2 is denoted as the ratio between the final and initial concentration (C/C_0)

[5] Ramalingam, G., Perumal, N., Priya, A.K., Rajendran, S. (2022). A review of graphene-based semiconductors for photocatalytic degradation of pollutants in wastewater. *Chemosphere*, 300 DOI: 10.1016/j.chemosphere.2022.134391.

[6] Kumar, S., Himanshi, Prakash, J., Verma, A., Suman, Jasrotia, R., Kandwal, A., Verma, R., Godara, S.K., Khan, M.A.M., Alshehri, S.M., Ahmed, J. (2023). A Review on Properties and Environmental Applications of Graphene and Its Derivative-Based Composites. *Catalysts*, 13(1), 111. DOI: 10.3390/catal13010111.

[7] Zhu, Y., Murali, S., Cai, W., Li, X., Suk, J.W., Potts, J.R., Ruoff, R.S. (2010). Graphene and graphene oxide: Synthesis, properties, and applications. *Advanced Materials*, 22(35), 3906–3924. DOI: 10.1002/adma.201001068.

[8] Chowdhury, S., Balasubramanian, R. (2014). Graphene/semiconductor nanocomposites (GSNs) for heterogeneous photocatalytic decolorization of wastewaters contaminated with synthetic dyes: A review. *Applied Catalysis B: Environmental*, 160–161, 307–324. DOI: 10.1016/j.apcatb.2014.05.035.

[9] Ganguly, P., Harb, M., Cao, Z., Cavallo, L., Breen, A., Dervin, S., Dionysiou, D.D., Pillai, S.C. (2019). 2D Nanomaterials for Photocatalytic Hydrogen Production. *ACS Energy Letters*, 4(7), 1687–1709. DOI: 10.1021/acsenergylett.9b00940.

[10] Geim, A.K., Novoselov, K.S. (2007). The rise of gra-phene. *Nature Materials*, 6, 183–191. DOI: 10.1038/nmat1849

[11] Zhang, N., Zhang, Y., Xu, Y.J. (2012). Recent progress on graphene-based photocatalysts: current status and future perspectives. *Nanoscale*, 4(19), 5792–5813. DOI: 10.1039/C2NR31480K.

[12] Ito, J., Nakamura, J., Natori, A. (2008). Semiconducting nature of the oxygen-adsorbed graphene sheet. *Journal of Applied Physics*, 103(11), 113712. DOI: 10.1063/1.2939270.

[13] Matsumoto, Y., Koinuma, M., Ida, S., Hayami, S., Taniguchi, T., Hatakeyama, K., Tateishi, H., Watanabe, Y., Amano, S. (2011). Photoreaction of graphene oxide nanosheets in water. *Journal of Physical Chemistry C*, 115(39), 19280–19286. DOI: 10.1021/jp206348s.

[14] Samriti, Manisha, Chen, Z., Sun, S., Prakash, J. (2022). Design and engineering of grapheme nanostructures as independent solar-driven photocatalysts for emerging applications in the field of energy and environment. *Mol. Syst. Des. Eng.* 7, 213–238. DOI: 10.1039/D1ME00179E

[15] Siong, V.L.E., Tai, X.H., Lee, K.M., Juan, J.C., Lai, C.W. (2020). Unveiling the enhanced photoelectrochemical and photocatalytic properties of reduced graphene oxide for photodegradation of methylene blue dye. *RSC Advances*, 10(62), 37905–37915. DOI: 10.1039/D0RA06703B.

[16] Siong, V.L.E., Tai, X.H., Lee, K.M., Juan, J.C., Lai, C.W. (2020). Unveiling the enhanced photoelectrochemical and photocatalytic properties of reduced graphene oxide for photodegradation of methylene blue dye. *RSC Advances*, 10(62), 37905–37915. DOI: 10.1039/d0ra06703b.

[17] Siong, V.L.E., Lee, K.M., Juan, J.C., Lai, C.W., Tai, X.H., Khe, C.S. (2019). Removal of methylene blue dye by solvothermally reduced graphene oxide: A metal-free adsorption and photodegradation method. *RSC Advances*, 9(64), 37686–37695. DOI: 10.1039/c9ra05793e.

[18] Krishnamoorthy, K., Mohan, R., Kim, S.J. (2011). Graphene oxide as a photocatalytic material. *Applied Physics Letters*, 98(24) DOI: 10.1063/1.3599453.

[19] Trinh, D.N., Viet, T.Q.Q., Nhu, T.H., Dat, N.M., Thinh, D.B., Hai, N.D., Tai, L.T., Oanh, D.T.Y., Khoi, V.H., Nam, H.M., Phong, M.T., Hieu, N.H. (2021). Binary TiO_2/reduced graphene oxide nanocomposite for improving methylene blue photodegradation. *Vietnam Journal of Chemistry*, 59(3), 395–404. DOI: 10.1002/vjch.202100009.

[20] Mohan, H., Ramalingam, V., Karthi, N., Malathidevi, S., Shin, T., Venkatachalam, J., Seralathan, K.K. (2021). Enhanced visible light-driven photocatalytic activity of reduced graphene oxide/cadmium sulfide composite: Methylparaben degradation mechanism and toxicity. *Chemosphere*, 264 DOI: 10.1016/j.chemosphere.2020.128481.

[21] Wang, C.Y., Wu, T., Lin, Y.W. (2019). Preparation and characterization of bismuth oxychloride/reduced graphene oxide for photocatalytic degradation of rhodamine B under white-light light-emitting-diode and sunlight irradiation. *Journal of Photochemistry and Photobiology A: Chemistry*, 371, 355–364. DOI: 10.1016/j.jphotochem.2018.11.043.

[22] Shen, J.H., Li, M.M., Chu, L.F., Guo, C.X., Guo, Y.J., Guo, Y.P. (2021). Effect mechanism of copper ions on photocatalytic activity of TiO_2/graphene oxide composites for phenol-4-sulfonic acid photodegradation. *Journal of Colloid and Interface Science*, 586, 563–575. DOI: 10.1016/j.jcis.2020.10.121.

[23] Hu, J., Li, H., Muhammad, S., Wu, Q., Zhao, Y., Jiao, Q. (2017). Surfactant-assisted hydrothermal synthesis of TiO_2/reduced graphene oxide nanocomposites and their photocatalytic performances. *Journal of Solid State Chemistry*, 253, 113–120. DOI: 10.1016/J.JSSC.2017.05.034.

[24] Prasad, C., Liu, Q., Tang, H., Yuvaraja, G., Long, J., Rammohan, A., Zyryanov, G. v. (2020). An overview of graphene oxide supported semiconductors based photocatalysts: Properties, synthesis and photocatalytic applications. *Journal of Molecular Liquids*, 297, 111826. DOI: 10.1016/j.molliq.2019.111826.

[25] Tayel, A., Ramadan, A.R., el Seoud, O.A. (2018). Titanium Dioxide/Graphene and Titanium Dioxide/Graphene Oxide Nanocomposites: Synthesis, Characterization and Photocatalytic Applications for Water Decontamination. *Catalysts,* 8 (11), 491. DOI: 10.3390/catal8110491.

[26] Chen, X., Mao, S.S. (2007). Titanium dioxide nanomaterials: Synthesis, properties, modifications and applications. *Chemical Reviews*, 107 (7), 2891–2959. DOI: 10.1021/cr0500535.

[27] Fundamentals and Applications of Nanomaterials - Zhen Guo, Li Tan - Google Books. https://books.google.com.my/books?hl=en&lr=&id=TEqEz0hKJOQC&oi=fnd&pg=PR3&ots=jnl6GE4Mh5&sig=DEraBcsLRRZeFHlPPVVtdyJsl74&redir_esc=y#v=onepage&q&f=false. Accessed 20 May 2022.

[28] The Chemistry of Nanomaterials: Synthesis, Properties and Applications - Google Books. https://books.google.com.my/books?hl=en&lr=&id=XjB43Kt-HXYC&oi=fnd&pg=PR5&ots=enKdRfVFrA&sig=0y_u_D0e9NHXXtLQ_uc0AqvD1Ig&redir_esc=y#v=onepage&q&f=false. Accessed 20 May 2022.

[29] Handbook of Hydrothermal Technology - K. Byrappa, Masahiro Yoshimura - Google Books. https://books.google.com.my/books?hl=en&lr=&id=vA5tXzLsHioC&oi=fnd&pg=PP1&ots=cypd3Sonhk&sig=C-neu2r-Bu3AArQELfrBBq9a6zM&redir_esc=y#v=onepage&q&f=false. Accessed 20 May 2022.

[30] Tong, Z., Yang, D., Shi, J., Nan, Y., Sun, Y., Jiang, Z. (2015). Three-Dimensional Porous Aerogel Constructed by g-C_3N_4 and Graphene Oxide Nanosheets with Excellent Visible-Light Photocatalytic Performance. *ACS Applied Materials and Interfaces*, 7(46), 25693–25701. DOI: 10.1021/acsami.5b09503

[31] Hu, J., Li, H., Muhammad, S., Wu, Q., Zhao, Y., Jiao, Q. (2017). Surfactant-assisted hydrothermal synthesis of TiO_2/reduced graphene oxide nanocomposites and their photocatalytic performances. Journal of Solid State Chemistry, 253, 113–120. DOI: 10.1016/j.jssc.2017.05.034

[32] Bie, C., Yu, H., Cheng, B., Ho, W., Fan, J., Yu, J. (2021). Design, Fabrication, and Mechanism of Nitrogen-Doped Graphene-Based Photocatalyst. *Advanced Materials*, 33(9), 2003521. DOI: 10.1002/adma.202003521.

[33] Wu, M.H., Li, L., Xue, Y.C., Xu, G., Tang, L., Liu, N., Huang, W.Y. (2018). Fabrication of ternary GO/g-C_3N_4/MoS_2 flower-like heterojunctions with enhanced photocatalytic activity for water remediation. *Applied Catalysis B: Environmental*, 228, 103–112. DOI: 10.1016/j.apcatb.2018.01.063.

[34] Wang, C., Cao, M., Wang, P., Ao, Y., Hou, J., Qian, J. (2014). Preparation of graphene–carbon nanotube–TiO_2 composites with enhanced photocatalytic activity for the removal of dye and Cr(VI). *Applied Catalysis A: General*, 473, 83–89. DOI: 10.1016/j.apcata.2013.12.028.

[35] Bajaj, N.S., Joshi, R.A. (2021). Energy materials: synthesis and characterization techniques. *Energy Materials: Fundamentals to Applications*, Chapter 3, 61–82. DOI: 10.1016/B978-0-12-823710-6.00019-4.

[36] Thambidurai, S., Gowthaman, P., Venkatachalam, M., Suresh, S. (2020). Natural sunlight assisted photocatalytic degradation of methylene blue by spherical zinc oxide nanoparticles prepared by facile chemical coprecipitation method. *Optik*, 207, 163865. DOI: 10.1016/j.ijleo.2019.163865

[37] Zhou, Y., Li, J., Liu, C., Huo, P., Wang, H. (2018). Construction of 3D porous g-C_3N_4/AgBr/rGO composite for excellent visible light photocatalytic activity. *Applied Surface Science*, 458, 586–596. DOI: 10.1016/j.apsusc.2018.07.121.

[38] Hench, L.L., West, J.K. (1990). The Sol-Gel Process. *Chemical Reviews*, 90(1), 33–72. DOI: 10.1021/cr00099a003.

[39] Xu, D., Li, L., He, R., Qi, L., Zhang, L., Cheng, B. (2018). Noble metal-free RGO/TiO_2 composite nanofiber with enhanced photocatalytic H_2-production performance. *Applied Surface Science*, 434, 620–625. DOI: 10.1016/j.apsusc.2017.10.192.

[40] Štengl, V., Bakardjieva, S., Grygar, T.M., Bludská, J., Kormunda, M. (2013). TiO_2-graphene oxide nanocomposite as advanced photocatalytic materials. *Chemistry Central Journal*, 7(1), 1–12. DOI: 10.1186/1752-153X-7-41.

[41] Park, C.Y., Kefayat, U., Vikram, N., Ghosh, T., Oh, W.C., Cho, K.Y. (2013). Preparation of novel CdS-graphene/TiO_2 composites with high photocatalytic activity for methylene blue dye under visible light. *Bulletin of Materials Science 2013 36:5*, 36(5), 869–876. DOI: 10.1007/S12034-013-0533-5.

[42] Tang, B., Chen, H., Peng, H., Wang, Z., Huang, W. (2018). Graphene Modified TiO_2 Composite Photocatalysts: Mechanism, Progress and Perspective. *Nanomaterials,* 8(2), 105. DOI: 10.3390/nano8020105.

[43] Faraldos, M., Bahamonde, A. (2017). Environmental applications of titania-graphene photocatalysts. *Catalysis Today*, 285, 13–28. DOI: 10.1016/j.cattod.2017.01.029.

[44] Karthik, V., Selvakumar, P., Senthil Kumar, P., Vo, D.V.N., Gokulakrishnan, M., Keerthana, P., Tamil Elakkiya, V., Rajeswari, R. (2021). Graphene-based materials for environmental applications: a review. *Environmental Chemistry Letters*, 19(5), 3631–3644. DOI: 10.1007/S10311-021-01262-3.

[45] Dutta, V., Singh, P., Shandilya, P., Sharma, S., Raizada, P., Saini, A.K., Gupta, V.K., Hosseini-Bandegharaei, A., Agarwal, S., Rahmani-Sani, A. (2019). Review on advances in photocatalytic water disinfection utilizing graphene and graphene derivatives-based nanocomposites. *Journal of Environmental Chemical Engineering*, 7(3), 103132. DOI: 10.1016/j.jece.2019.103132.

[46] Zhao, G., Li, X., Huang, M., Zhen, Z., Zhong, Y., Chen, Q., Zhao, X., He, Y., Hu, R., Yang, T., Zhang, R., Li, C., Kong, J., Xu, J. bin, Ruoff, R.S., Zhu, H. (2017). The physics and chemistry of graphene-on-surfaces. *Chemical Society Reviews*, 46 (15), 4417–4449. DOI: 10.1039/C7CS00256D.

[47] Chen, D., Cheng, Y., Zhou, N., Chen, P., Wang, Y., Li, K., Huo, S., Cheng, P., Peng, P., Zhang, R., Wang, L., Liu, H., Liu, Y., Ruan, R. (2020). Photocatalytic degradation of organic pollutants using TiO_2-based photocatalysts: A review. *Journal of Cleaner Production*, 268, 121725. DOI: 10.1016/j.jclepro.2020.121725.

[48] Chen, L., He, J., Liu, Y., Chen, P., Au, C.T., Yin, S.F. (2016). Recent advances in bismuth-containing photocatalysts with heterojunctions. *Chinese Journal of Catalysis*, 37(6), 780–791. DOI: 10.1016/S1872-2067(15)61061-0.

[49] Low, J., Yu, J., Jaroniec, M., Wageh, S., Al-Ghamdi, A.A. (2017). Heterojunction Photocatalysts. *Advanced Materials*, 29(20), 1601694. DOI: 10.1002/adma.201601694.

[50] Li, X., Shen, R., Ma, S., Chen, X., Xie, J. (2018). Graphene-based heterojunction photocatalysts. *Applied Surface Science*, 430, 53–107. DOI: 10.1016/j.apsusuc.2017.08.194.

[51] Zhang, W., Guo, H., Sun, H., Zeng, R. (2017). Constructing ternary polyaniline-graphene-TiO_2 hybrids with enhanced photoelectrochemical performance in photo-generated cathodic protection. *Applied Surface Science*, 410, 547–556. DOI: 10.1016/j.apsusc.2017.03.133.

[52] Miao, J., Xie, A., Li, S., Huang, F., Cao, J., Shen, Y. (2016). A novel reducing graphene/polyaniline/cuprous oxide composite hydrogel with unexpected photocatalytic activity for the degradation of Congo red. *Applied Surface Science*, 360, 594–600. DOI: 10.1016/j.apsusc.2015.11.005.

[53] Tang, B., Chen, H., He, Y., Wang, Z., Zhang, J., Wang, J. (2017). Influence from defects of three-dimensional graphene network on photocatalytic performance of composite photocatalyst. *Composites Science and Technology*, 150, 54–64. DOI: 10.1016/j.compscitech.2017.07.007.

[54] Sun, Y., Wang, X., Tang, B., Ban, J., He, Y., Huang, W., Tao, C., Luo, H., Sun, J. (2017). Three-dimensional graphene networks modified photocatalyst with high performance under visible-light irradiation. *Materials Letters*, 189, 54–57. DOI: 10.1016/j.matlet.2016.06.113.

[55] Kaplan, R., Erjavec, B., Dražić, G., Grdadolnik, J., Pintar, A. (2016). Simple synthesis of anatase/rutile/brookite TiO_2 nanocomposite with superior mineralization potential for photocatalytic degradation of water pollutants. *Applied Catalysis B: Environmental*, 181, 465–474. DOI: 10.1016/j.apcatb.2015.08.027.

[56] Xiong, Z, Lei, Z., Li, Y., Dong, L., Zhao, Y., Zhang, J. (2018). A review on modification of facet-engineered TiO_2 for photocatalytic CO_2 reduction. *Journal of Photochemistry and Photobiology C: Photochemistry Reviews*, 36, 24-47. DOI: 10.1016/j.jphotochemrev.2018.07.002.

[57] Kavitha, M.K., Gopinath, P., John, H. (2015). Reduced graphene oxide–ZnO self-assembled films: tailoring the visible light photoconductivity by the intrinsic defect states in ZnO. *Physical Chemistry Chemical Physics*, 17(22), 14647–14655. DOI: 10.1039/C5CP01318F.

[58] Sharma, M., Behl, K., Nigam, S., Joshi, M. (2018). TiO_2-GO nanocomposite for photocatalysis and environmental applications: A green synthesis approach. *Vacuum*, 156, 434–439. DOI: 10.1016/j.vacuum.2018.08.009.

[59] Zhang, H., Lv, X., Li, Y., Wang, Y., Li, J. (2010). P25-graphene composite as a high performance photocatalyst. *ACS Nano*, 4(1), 380–386. DOI: 10.1021/nn901221k.

[60] Bukhari, K., Ahmad, N., Sheikh, I.A., Akram, T.M. (2019). Effects of Different Parameters on Photocatalytic Oxidation of Slaughterhouse Wastewater Using TiO_2 and Silver-Doped TiO_2 Nanoparticles. *Polish Journal of Environmental Studies*, 28(3), 1591–1600. DOI: 10.15244/pjoes/90635.

[61] Rozman, N., Tobaldi, D.M., Cvelbar, U., Puliyalil, H., Labrincha, J.A., Legat, A., Škapin, A.S. (2019). Hydrothermal Synthesis of Rare-Earth Modified Titania: Influence on Phase Composition, Optical Properties, and Photocatalytic Activity. *Materials 2019, Vol 12, Page 713*, 12(5), 713. DOI: 10.3390/MA12050713.

[62] Gohr, M.S., Hafez, H.S., Saif, M.M., Soliman, H.M.A., Abdel-Mottaleb, M.S.A. (2020). Facile Hydrothermal Synthesis of Sm and Eu doped TiO_2/Graphene Oxide Nanocomposites for Photocatalytic Applications. *Egyptian Journal of Chemistry*, 63(4), 1359–1382. DOI: 10.21608/ejchem.2019.15112.1914.

[63] Sakthivel, S., Shankar, M. v., Palanichamy, M., Arabindoo, B., Bahnemann, D.W., Murugesan, V. (2004). Enhancement of photocatalytic activity by metal deposition: characterisation and photonic efficiency of Pt, Au and Pd deposited on TiO_2 catalyst. *Water Research*, 38(13), 3001–3008. DOI: 10.1016/j.watres.2004.04.046.

[64] Umebayashi, T., Yamaki, T., Itoh, H., Asai, K. (2002). Band gap narrowing of titanium dioxide by sulfur doping. *Applied Physics Letters*, 81(3), 454. DOI: 10.1063/1.1493647.

[65] Asahi, R., Morikawa, T., Ohwaki, T., Aoki, K., Taga, Y. (2001). Visible-Light Photocatalysis in Nitrogen-Doped Titanium Oxides. *Science*, 293(5528), 269–271. DOI: 10.1126/science.1061051.

[66] Shang, X., Zhang, M., Wang, X., Yang, Y. (2014). Sulphur, nitrogen-doped TiO_2/graphene oxide composites as a high performance photocatalyst. *Journal of Experimental Nanoscience*, 9(7), 749–761. DOI: 10.1080/17458080.2012.713127.

[67] Yu, M., Yu, T., Chen, S., Guo, Z., Seok, I. (2020). A Facile Synthesis of Ag/TiO_2/rGO Nanocomposites with Enhanced Visible Light Photocatalytic Activity. *ES Materials & Manufacturing*, 7, 64-69. DOI: 10.30919/esmm5f712

[68] Isari, A.A., Payan, A., Fattahi, M., Jorfi, S., Kakavandi, B. (2018). Photocatalytic degradation of rhodamine B and real textile wastewater using Fe-doped TiO_2 anchored on reduced graphene oxide (Fe-TiO_2/rGO): Characterization and feasibility, mechanism and pathway studies. *Applied Surface Science*, 462, 549–564. DOI: 10.1016/j.apsusc.2018.08.133.

[69] Sun, S., Ding, J., Bao, J., Gao, C., Qi, Z., Yang, X., He, B., Li, C. (2012). Photocatalytic degradation of gaseous toluene on Fe-TiO_2 under visible light irradiation: A study on the structure, activity and deactivation mechanism. *Applied Surface Science*, 258(12), 5031–5037. DOI: 10.1016/j.apsusc.2012.01.075.

[70] Farhangi, N., Chowdhury, R.R., Medina-Gonzalez, Y., Ray, M.B., Charpentier, P.A. (2011). Visible light active Fe doped TiO_2 nanowires grown on graphene using supercritical CO_2. *Applied Catalysis B: Environmental*, 110, 25–32. DOI: 10.1016/j.apcatb.2011.08.012.

[71] Hasan, M.R., Lai, C.W., Bee Abd Hamid, S., Jeffrey Basirun, W. (2014). Effect of Ce doping on RGO-TiO_2 nanocomposite for high photoelectrocatalytic behavior. *International Journal of Photoenergy*, 2014 DOI: 10.1155/2014/141368.

[72] Behera, L., Barik, B., Mohapatra, S. (2021). Improved photodegradation and antimicrobial activity of hydrothermally synthesized 0.2Ce-TiO_2/RGO under visible light. *Colloids and Surfaces A: Physicochemical and Engineering Aspects*, 620, 126553. DOI: 10.1016/j.colsurfa.2021.126553.

[73] Bao, H. van, Dat, N.M., Giang, N.T.H., Thinh, D.B., Tai, L.T., Trinh, D.N., Hai, N.D., Khoa, N.A.D., Huong, L.M., Nam, H.M., Phong, M.T., Hieu, N.H. (2021). Behavior of ZnO-doped TiO_2/rGO nanocomposite for water treatment enhancement. *Surfaces and Interfaces*, 23, 100950. DOI: 10.1016/j.surfin.2021.100950.

[74] Sutter, P.W., Flege, J.I., Sutter, E.A. (2008). Epitaxial graphene on ruthenium. *Nature Materials*, 7(5), 406–411. DOI: 10.1038/nmat2166.

[75] Marta, B., Leordean, C., Istvan, T., Botiz, I., Astilean, S. (2016). Efficient etching-free transfer of high quality, large-area CVD grown graphene onto polyvinyl alcohol films. *Applied Surface Science*, 363, 613–618. DOI: 10.1016/j.apsusc.2015.11.265.

[76] Berger, C., Song, Z., Li, X., Wu, X., Brown, N., Naud, C., Mayou, D., Li, T., Hass, J., Marchenkov, A.N., Conrad, E.H., First, P.N., de Heer, W.A. (2006). Electronic Confinement and Coherence in Patterned Epitaxial Graphene. *Science*, 312(5777), 1191–1196. DOI: 10.1126/science.1125925.

[77] Iliut, M., Gabudean, A.M., Leordean, C., Simon, T., Teodorescu, C.M., Astilean, S. (2013). Riboflavin enhanced fluorescence of highly reduced graphene oxide. *Chemical Physics Letters*, 586, 127–131. DOI: 10.1016/j.cplett.2013.09.032.

[78] Iliut, M., Leordean, C., Canpean, V., Teodorescu, C.M., Astilean, S. (2013). A new green, ascorbic acid-assisted method for versatile synthesis of Au–graphene hybrids as efficient surface-enhanced Raman scattering platforms. *Journal of Materials Chemistry C*, 1(26), 4094–4104. DOI: 10.1039/C3TC30177J.

[79] Albiter, E., Merlano, A.S., Rojas, E., Barrera-Andrade, J.M., Salazar, Á., Valenzuela, M.A. (2020). Synthesis, Characterization, and Photocatalytic Performance of ZnO–Graphene Nanocomposites: A Review. *Journal of Composites Science*, 5(1), 4. DOI: 10.3390/jcs5010004.

[80] Moezzi, A., McDonagh, A.M., Cortie, M.B. (2012). Zinc oxide particles: Synthesis, properties and applications. *Chemical Engineering Journal*, 185–186, 1–22. DOI: 10.1016/j.cej.2012.01.076.

[81] Samadi, M., Zirak, M., Naseri, A., Kheirabadi, M., Ebrahimi, M., Moshfegh, A.Z. (2019). Design and tailoring of one-dimensional ZnO nanomaterials for photocatalytic degradation of organic dyes: a review. *Research on Chemical Intermediates*, 45(4), 2197–2254. DOI: 10.1007/s11164-018-03729-5.

[82] Wojnarowicz, J., Chudoba, T., Lojkowski, W. (2020). A Review of Microwave Synthesis of Zinc Oxide Nanomaterials: Reactants, Process Parameters and Morphologies. *Nanomaterials*, 10(6), 1086. DOI: 10.3390/nano10061086.

[83] Yaqoob, A.A., Noor, N.H.B.M., Serrà, A., Ibrahim, M.N.M. (2020). Advances and Challenges in Developing Efficient Graphene Oxide-Based ZnO Photocatalysts for Dye Photo-Oxidation. *Nanomaterials,* 10 (5), 932. DOI: 10.3390/nano10050932.

[84] Raizada, P., Sudhaik, A., Singh, P. (2019). Photocatalytic water decontamination using graphene and ZnO coupled photocatalysts: A review. *Materials Science for Energy Technologies*, 2(3), 509–525. DOI: 10.1016/j.mset.2019.04.007.

[85] Yang, M.Q., Xu, Y.J. (2013). Basic principles for observing the photosensitizer role of graphene in the graphene-semiconductor composite photocatalyst from a case study on graphene-ZnO. *Journal of Physical Chemistry C*, 117(42), 21724–21734. DOI: 10.1021/jp408400c.

[86] Ida, S., Takashiba, A., Koga, S., Hagiwara, H., Ishihara, T. (2014). Potential gradient and photocatalytic activity of an ultrathin p-n junction surface prepared with two-dimensional semiconducting nanocrystals. *Journal of the American Chemical Society*, 136(5), 1872–1878. DOI: 10.1021/ja409465k.

[87] Albiter, E., Merlano, A.S., Rojas, E., Barrera-Andrade, J.M., Salazar, Á., Valenzuela, M.A. (2021). Synthesis, Characterization, and Photocatalytic Performance of ZnO–Graphene Nanocomposites: A Review. *Journal of Composites Science,* 5(1), 4. DOI: 10.3390/jcs5010004.

[88] Yu, H., Chen, F., Chen, F., Wang, X. (2015). In situ self-transformation synthesis of g-C_3N_4-modified CdS heterostructure with enhanced photocatalytic activity. *Applied Surface Science*, 358, 385–392. DOI: 10.1016/j.apsusc.2015.06.074.

[89] Mohan, H., Ramalingam, V., Karthi, N., Malathidevi, S., Shin, T., Venkatachalam, J., Seralathan, K.K. (2021). Enhanced visible light-driven photocatalytic activity of reduced graphene oxide/cadmium sulfide composite: Methylparaben degradation mechanism and toxicity. *Chemosphere*, 264, 128481. DOI: 10.1016/j.chemosphere.2020.128481.

[90] Cao, H.L., Cai, F.Y., Yu, K., Zhang, Y.Q., Lü, J., Cao, R. (2019). Photocatalytic Degradation of Tetracycline Antibiotics over CdS/Nitrogen-Doped-Carbon Composites Derived from in Situ Carbonization of Metal-Organic Frameworks. *ACS Sustainable Chemistry and Engineering*, 7(12), 10847–10854. DOI: 10.1021/acssuschemeng.9b01685.

[91] Cao, H.L., Cai, F.Y., Yu, K., Zhang, Y.Q., Lü, J., Cao, R. (2019). Photocatalytic Degradation of Tetracycline Antibiotics over CdS/Nitrogen-Doped-Carbon Composites Derived from in Situ Carbonization of Metal-Organic Frameworks. *ACS Sustainable Chemistry and Engineering*, 7(12), 10847–10854. DOI: 10.1021/acssuschemeng.9b01685.

[92] Antoniadou, M., Daskalaki, V.M., Balis, N., Kondarides, D.I., Kordulis, C., Lianos, P. (2011). Photocatalysis and photoelectrocatalysis using (CdS-ZnS)/TiO_2 combined photocatalysts. *Applied Catalysis B: Environmental*, 107(1–2), 188–196. DOI: 10.1016/j.apcatb.2011.07.013.

[93] Khatter, J., Chauhan, R.P. (2020). Effect of temperature on properties of cadmium sulfide nanostructures synthesized by solvothermal method. *Journal of Materials Science: Materials in Electronics*, 31(3), 2676–2685. DOI: 10.1007/S10854-019-02807-7.

[94] Sharma, S., Dutta, V., Raizada, P., Hosseini-Bandegharaei, A., Singh, P., Nguyen, V.H. (2020). Tailoring cadmium sulfide-based photocatalytic nanomaterials for water decontamination: a review. *Environmental Chemistry Letters,* 19(1), 271–306. DOI: 10.1007/S10311-020-01066-X.

[95] Peng, T., Li, K., Zeng, P., Zhang, Q., Zhang, X. (2012). Enhanced photocatalytic hydrogen production over graphene oxide-cadmium sulfide nanocomposite under visible light irradiation. *Journal of Physical Chemistry C*, 116(43), 22720–22726. DOI: 10.1021/jp306947d.

[96] Shi, J.W., Yan, X., Cui, H.J., Zong, X., Fu, M.L., Chen, S., Wang, L. (2012). Low-temperature synthesis of CdS/TiO_2 composite photocatalysts: Influence of synthetic procedure on photocatalytic activity under visible light. *Journal of Molecular Catalysis A: Chemical*, 356, 53–60. DOI: 10.1016/j.molcata.2012.01.001.

[97] Sagadevan, S., Chowdhury, Z.Z., Johan, M.R. bin, Aziz, F.A., Roselin, L.S., Hsu, H.L., Selvin, R. (2019). Synthesis, characterization and electrochemical properties of cadmium sulfide – Reduced graphene oxide nanocomposites. *Results in Physics*, 12, 878–885. DOI: 10.1016/j.rinp.2018.12.058.

[98] Ye, H., Park, H.S., Bard, A.J. (2011). Screening of electrocatalysts for photoelectrochemical water oxidation on W-doped BiVO4 photocatalysts by scanning electrochemical microscopy. *Journal of Physical Chemistry C*, 115(25), 12464–12470. DOI: 10.1021/jp200852c.

[99] Chen, Z., Liu, S., Yang, M.Q., Xu, Y.J. (2013). Synthesis of uniform CdS nanospheres/graphene hybrid nanocomposites and their application as visible light photocatalyst for selective reduction of nitro organics in water. *ACS Applied Materials and Interfaces*, 5(10), 4309–4319. DOI: 10.1021/am4010286.

[100] Zhang, L., Yang, J., Zhao, X., Xiao, X., Sun, F., Zuo, X., Nan, J. (2020). Small-molecule surface-modified bismuth-based semiconductors as a new class of visible-light-driven photocatalytic materials: Structure-dependent photocatalytic properties and photosensitization mechanism. *Chemical Engineering Journal*, 380, 122546. DOI: 10.1016/j.cej.2019.122546.

[101] Pattnaik, S.P., Behera, A., Martha, S., Acharya, R., Parida, K. (2018). Synthesis, photoelectrochemical properties and solar light-induced photocatalytic activity of bismuth ferrite nanoparticles. *Journal of Nanoparticle Research*, 20(1), 1–15. DOI: 10.1007/S11051-017-4110-5.

[102] Usman, M., Humayun, M., Shah, S.S., Ullah, H., Tahir, A.A., Khan, A., Ullah, H. (2021). Bismuth-Graphene Nanohybrids: Synthesis, Reaction Mechanisms, and Photocatalytic Applications - A Review. *Energies,* 14 (8), 2281. DOI: 10.3390/en14082281.

[103] Baumert, B.A. (1995). Barium potassium bismuth oxide: A review. *Journal of Superconductivity,* 8 (1), 175–181. DOI: 10.1007/bf00732261.

[104] Fang, W., Shangguan, W. (2019). A review on bismuth-based composite oxides for photocatalytic hydrogen generation. *International Journal of Hydrogen Energy*, 44(2), 895–912. DOI: 10.1016/j.ijhydene.2018.11.063.

[105] Chen, Z., Niu, F., Huang, X., Gao, T., Huang, Q., Qin, L., Huang, Y. (2015). A review: Preparation of bismuth ferrite nanoparticles and its applications in visible-light induced photocatalyses. *Rev. Adv. Mater. Sci.*, 40, 97–109.

[106] Sharma, K., Dutta, V., Sharma, S., Raizada, P., Hosseini-Bandegharaei, A., Thakur, P., Singh, P. (2019). Recent advances in enhanced photocatalytic activity of bismuth oxyhalides for efficient photocatalysis of organic pollutants in water: A review. *Journal of Industrial and Engineering Chemistry*, 78, 1–20. DOI: 10.1016/j.jiec.2019.06.022.

[107] Zhang, L., Li, Y., Li, Q., Fan, J., Carabineiro, S.A.C., Lv, K. (2021). Recent advances on Bismuth-based Photocatalysts: Strategies and mechanisms. *Chemical Engineering Journal*, 419, 129484. DOI: 10.1016/j.cej.2021.129484.

[108] Selvaraj, R., Qi, K., Al-Kindy, S.M.Z., Sillanpää, M., Kim, Y., Tai, C.W. (2014). A simple hydrothermal route for the preparation of HgS nanoparticles and their photocatalytic activities. *RSC Advances*, 4(30), 15371–15376. DOI: 10.1039/C4RA00483C.

[109] Wang, C.Y., Wu, T., Lin, Y.W. (2019). Preparation and characterization of bismuth oxychloride/reduced graphene oxide for photocatalytic degradation of rhodamine B under white-light light-emitting-diode and sunlight irradiation. *Journal of Photochemistry and Photobiology A: Chemistry*, 371, 355–364. DOI: 10.1016/j.jphotochem.2018.11.043.

[110] Sun, D., Li, J., Feng, Z., He, L., Zhao, B., Wang, T., Li, R., Yin, S., Sato, T. (2014). Solvothermal synthesis of BiOCl flower-like hierarchical structures with high photocatalytic activity. *Catalysis Communications*, 51, 1–4. DOI: 10.1016/j.catcom.2014.03.004.

[111] Hu, J., Fan, W., Ye, W., Huang, C., Qiu, X. (2014). Insights into the photosensitivity activity of BiOCl under visible light irradiation. *Applied Catalysis B: Environmental*, 158–159, 182–189. DOI: 10.1016/j.apcatb.2014.04.019.

[112] Lin, W., Yu, X., Zhu, Y., Zhang, Y. (2018). Graphene oxide/BiOCl nanocomposite films as efficient visible light photocatalysts. *Frontiers in Chemistry*, 6, 274. DOI: 10.3389/fchem.2018.00274.

[113] Upadhyay, R.K., Soin, N., Bhattacharya, G., Saha, S., Barman, A., Roy, S.S. (2015). Grape extract assisted green synthesis of reduced graphene oxide for water treatment application. *Materials Letters*, 160, 355–358. DOI: 10.1016/j.matlet.2015.07.144.

[114] Hu, G., Tang, B. (2013) Photocatalytic mechanism of graphene / titanate nanotubes photocatalyst under visible-light irradiation. *Materials Chemistry and Physics*, 138 (2–3), 608–614, DOI: 10.1016/j.matchemphys.2012.12.027.

[115] Scarpelli, F., Mastropietro, T.F., Poerio, T., Godbert, N. (2018). Mesoporous TiO_2 Thin Films: State of the Art. In (D.F. Yang (Editor)) *Titanium Dioxide - Material for a Sustainable Environment*. DOI: 10.5772/intechopen.74244

[116] Modan, E.M., Plaiasu, A.G. (2020). Advantages and Disadvantages of Chemical Methods in the Elaboration of Nanomaterials. *The Annals of "Dunarea de Jos" University of Galati Fascicle IX, Metallurgy and Materials Science*, 43(1), 53–60. DOI: 10.35219/mms.2020.1.08.

[117] Głowniak, S., Szczęśniak B., Choma J., Jaroniec M. (2021). Mechanochemistry: Toward green synthesis of metal–organic frameworks. *Materials Today*, 46, 109-124. DOI: 10.1016/j.mattod.2021.01.008

[118] Sayadi, M.H., Homaeigohar, S., Rezaei, A., Shekari, H. (2020). Bi/SnO_2/TiO_2-graphene nanocomposite photocatalyst for solar visible light–induced photodegradation of pentachlorophenol. *Environmental Science and Pollution Research,* 28(12), 15236–15247. DOI: 10.1007/S11356-020-11708-W.

[119] Zhang, H., Xu, P., Du, G., Chen, Z., Oh, K., Pan, D., Jiao, Z. (2010). A facile one-step synthesis of TiO_2/graphene composites for photodegradation of methyl orange. *Nano Research,* 4(3), 274–283. DOI: 10.1007/S12274-010-0079-4.

[120] Alsharaeh, E.H., Bora, T., Soliman, A., Ahmed, F., Bharath, G., Ghoniem, M.G., Abu-Salah, K.M., Dutta, J. (2017). Sol-Gel-Assisted Microwave-Derived Synthesis of Anatase Ag/TiO_2/GO Nanohybrids toward Efficient Visible Light Phenol Degradation. *Catalysts,* 7(5), 133. DOI: 10.3390/catal7050133.

[121] Li, T., Gao, Y., Zhou, J., Zhang, M., Fu, X., Liu, F. (2019). A Membrane Modified with Nitrogen-Doped TiO_2/Graphene Oxide for Improved Photocatalytic Performance. *Applied Sciences* 9(5), 855. DOI: 10.3390/app9050855.

[122] Garrafa-Gálvez, H.E., Alvarado-Beltrán, C.G., Almaral-Sánchez, J.L., Hurtado-Macías, A., Garzon-Fontecha, A.M., Luque, P.A., Castro-Beltrán, A. (2019). Graphene role in improved solar photocatalytic performance of TiO_2-RGO nanocomposite. *Chemical Physics*, 521, 35–43. DOI: 10.1016/j.chemphys.2019.01.013.

[123] Wang, H., Wang, G., Zhang, Y., Ma, Y., Wu, Z., Gao, D., Yang, R., Wang, B., Qi, X., Yang, J. (2019). Preparation of RGO/TiO_2/Ag Aerogel and Its Photodegradation Performance in Gas Phase Formaldehyde. *Scientific Reports,* 9(1), 1–12. DOI: 10.1038/s41598-019-52541-7.

[124] Bao, H. van, Dat, N.M., Giang, N.T.H., Thinh, D.B., Tai, L.T., Trinh, D.N., Hai, N.D., Khoa, N.A.D., Huong, L.M., Nam, H.M., Phong, M.T., Hieu, N.H. (2021). Behavior of ZnO-doped TiO_2/rGO nanocomposite for water treatment enhancement. *Surfaces and Interfaces*, 23, 100950. DOI: 10.1016/j.surfin.2021.100950.

[125] Behera, L., Barik, B., Mohapatra, S. (2021). Improved photodegradation and antimicrobial activity of hydrothermally synthesized 0.2Ce-TiO_2/RGO under visible light. *Colloids and Surfaces A: Physicochemical and Engineering Aspects*, 620, 126553. DOI: 10.1016/j.colsurfa.2021.126553.

[126] Sun, X., Ji, S., Wang, M., Dou, J., Yang, Z., Qiu, H., Kou, S., Ji, Y., Wang, H. (2020). Fabrication of porous TiO_2-RGO hybrid aerogel for high-efficiency, visible-light photodegradation of dyes. *Journal of Alloys and Compounds*, 819, 153033. DOI: 10.1016/j.jallcom.2019.153033.

[127] Babu, S.G., Karthik, P., John, M.C., Lakhera, S.K., Ashokkumar, M., Khim, J., Neppolian, B. (2019). Synergistic effect of sono-photocatalytic process for the degradation of organic pollutants using CuO-TiO_2/rGO. *Ultrasonics Sonochemistry*, 50, 218–223. DOI: 10.1016/j.ultsonch.2018.09.021.

[128] Kang, S., Pawar, R.C., Pyo, Y., Khare, V., Lee, C.S. (2016). Size-controlled BiOCl–RGO composites having enhanced photodegradative properties. *Journal of Experimental Nanoscience*, 11 (4), 259-275. DOI: 10.1080/17458080.2015.1047420

[129] Dong, S., Pi, Y., Li, Q., Hu, L., Li, Y., Han, X., Wang, J., Sun, J. (2016). Solar photocatalytic degradation of sulfanilamide by BiOCl/reduced graphene oxide nanocomposites: Mechanism and degradation pathways. *Journal of Alloys and Compounds*, 663, 1–9. DOI: 10.1016/j.jallcom.2015.12.027.

[130] Zheng, X., Yuan, J., Shen, J., Liang, J., Che, J., Tang, B., He, G., Chen, H. (2019). A carnation-like rGO/$Bi_2O_2CO_3$/BiOCl composite: efficient photocatalyst for the degradation of ciprofloxacin. *Journal of Materials Science: Materials in Electronics*, 30(6), 5986–5994. DOI: 10.1007/S10854-019-00898-W.

[131] Xue, B., Zou, Y. (2018). High photocatalytic activity of ZnO–graphene composite. *Journal of Colloid and Interface Science*, 529, 306–313. DOI: 10.1016/j.jcis.2018.04.040.

[132] Wang, H., Peng, D., Chen, T., Chang, Y., Dong, S. (2016). A novel photocatalyst AgBr/ZnO/RGO with high visible light photocatalytic activity. *Ceramics International*, 42(3), 4406–4412. DOI: 10.1016/j.ceramint.2015.11.124